

Rossby Wave Instability in Astrophysical Discs

R.V.E. Lovelace[‡] and M.M. Romanova[§]

Department of Astronomy, Cornell University, Ithaca, N.Y. 14853, USA

Abstract.

A brief review is given of the Rossby wave instability (RWI) in astrophysical discs. In non-self-gravitating discs, around for example a newly forming stars, the instability can be triggered by an axisymmetric bump at some radius r_0 in the disc surface mass-density. It gives rise to exponentially growing non-axisymmetric perturbation [$\propto \exp(im\phi)$, $m = 1, 2, \dots$] in the vicinity of r_0 consisting of *anticyclonic* vortices. These vortices are regions of high pressure and consequently act to trap dust particles which in turn can facilitate planetesimal growth in proto-planetary discs. The Rossby vortices in the discs around stars and black holes may cause the observed quasi-periodic modulations of the disc's thermal emission.

Keywords: Instabilities; Shear flows; Astrophysical flows.

[‡] lovelace@astro.cornell.edu

[§] romanova@astro.cornell.edu

1. Introduction

The theory of the Rossby wave instability (RWI) in accretion discs was developed by Lovelace *et al* (1999) and Li *et al* (2000) for thin Keplerian discs with negligible self-gravity and earlier by Lovelace and Hohlfeld (1978) for thin disc galaxies where the self-gravity may or may not be important and where the rotation is in general non-Keplerian. In the first case the instability can occur if there is an axisymmetric bump (as a function of radius) in the inverse potential vorticity

$$\mathcal{L}(r) = \frac{\Sigma S^{2/\gamma}}{2(\nabla \times \mathbf{u}) \cdot \hat{\mathbf{z}}}, \quad (1)$$

at some radius r_0 , where Σ is the surface mass density of the disc, $\mathbf{u} \approx r\Omega(r)\hat{\phi}$ is the flow velocity of the disc, $\Omega(r) \approx (GM_*/r^3)^{1/2}$ is the angular velocity of the flow (with M_* the mass of the central star), S is the specific entropy of the gas, and γ is the specific heat ratio. The approximations involve the neglect of the relatively small radial pressure force (see Sec. 3). Note that \mathcal{L} is related to the inverse of the *vortensity* which is defined as $(\nabla \times \mathbf{u})_z/\Sigma$. A sketch of a bump in $\mathcal{L}(r)$ is shown in Figure 1.

Rossby waves are important in planetary atmospheres and oceans and are also known as *planetary waves* (see Rossby *et al* 1939; Brekhovskikh and Goncharov 1993; Chelton and Schlax 1996; Lindzen 2005). These waves have a significant role in the transport of heat from equatorial to polar regions of the Earth. They may have a role in the formation of the long-lived (> 300 yr) Great Red Spot on Jupiter which is an anticyclonic vortex (e.g., Marcus 1993). The Rossby waves have the notable property of having the phase velocity opposite to the direction of motion of the atmosphere or

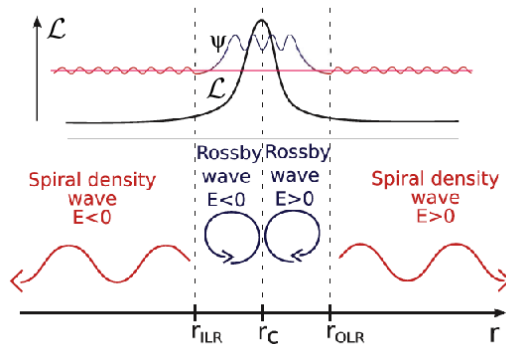


Figure 1. Schematic view of the Rossby wave instability with the two propagating regions for the Rossby waves, and in between the evanescent regions close to the inner and outer Lindblad resonant radii, (r_{ILR} and r_{OLR}), respectively, adapted from Meheut *et al* 2013). The radii of these Lindblad resonances are given by the equations $\omega = m\Omega(r_{\text{LR}}) \pm \kappa(r_{\text{LR}})$, where $\kappa(r)$ is the radial epicyclic frequency which is approximately equal to $\Omega(r)$ for a Keplerian disc. The corotation radius r_{C} is the radius where $\omega = m\Omega(r_{\text{C}})$.

disc in the comoving frame of the fluid (Brekhovskikh and Goncharov 1993; Lovelace *et al* 1999).

Section 2 summarizes the linear theory, Sec. 3 describes dust trapping in vortices, Sec. 4 is on vortices formed at the radial margins of the dead zone, Sec. 5 is on vortices due to planet induced gap edges, Sec. 6 is on the saturation and merging of vortices, Sec. 7 is on the influence of a large-scale magnetic field, Sec. 8 is on vortices in self-gravitating discs, and Sec. 9 gives a brief conclusion.

2. Schrödinger-like equation for perturbation

Linearization of the Euler and continuity equations for a thin fluid disc with perturbations proportional to $f(r) \exp(im\phi - i\omega t)$ (with azimuthal mode number $m = 1, 2, \dots$ and angular frequency ω) leads to a Schrödinger-like equation for the enthalpy perturbation $\psi = \delta p / \rho$,

$$\frac{d^2\psi}{dr^2} = V_{\text{eff}}(r) \psi . \quad (2)$$

The effective potential well $V_{\text{eff}}(r)$ is closely related to $\mathcal{L}(r)$: If the height of the bump in $\mathcal{L}(r)$ is too small the potential well is shallow and there are no ‘bound Rossby wave states’ in the well. On the other hand for a sufficiently large bump in $\mathcal{L}(r)$ the potential V_{eff} is sufficiently deep to have a bound state. The condition for there to be just one bound state allows one to solve for the imaginary part of the wave frequency, $\omega_i = \Im(\omega)$ which is the growth rate of the instability (Lovelace *et al.* 1999). For moderate strength bumps (with fractional amplitudes $\Delta\Sigma/\Sigma \lesssim 0.2$), the growth rates are of the order of $\omega_i = (0.1 - 0.2)\Omega(r_0)$. The real part of the wave frequency $\omega_r = \Re(\omega)$ is approximately $m\Omega(r_0)$.

A more complete analysis (Tagger 2001; Tsang and Lai 2008; Lai and Tsang 2009) reveals that the Rossby wave is not completely trapped in the potential well V_{eff} , but leaks outward across a forbidden region at an outer Lindblad resonance (at r_{OLR} indicated in Figure 1) and inward across another forbidden region at an inner Lindblad resonance (at r_{ILR}). Once the waves cross the forbidden regions they propagate as spiral density wave. The full expression for the effective potential for a thin *homentropic* ($S = \text{const}$) disc is

$$V_{\text{eff}} = \frac{2m\Omega}{r(\Delta\omega)} \frac{d}{dr} \left[\ln \left(\frac{\Omega\Sigma}{\kappa^2 - (\Delta\omega)^2} \right) \right] + \frac{m^2}{r^2} + \frac{\kappa^2 - (\Delta\omega)^2}{c_s^2} , \quad (3)$$

where $\Delta\omega \equiv \omega - m\Omega$ is the Doppler shifted wave frequency in the reference frame moving with the disc matter, c_s is the sound speed in the disc, and κ is the radial epicyclic angular frequency, with $\kappa^2 = r^{-3}d\ell^2/dr$ and $\ell = ru_\phi$ the specific angular momentum (Meheut *et al* 2013). Figure 2 shows the effective potential for sample cases. Note that the inward propagating waves with $\omega_r < m\Omega(r)$ have negative energy ($E < 0$) whereas the outward propagating waves with $\omega_r > m\Omega(r)$ have positive energy ($E > 0$) (e.g., Meheut *et al* 2013).

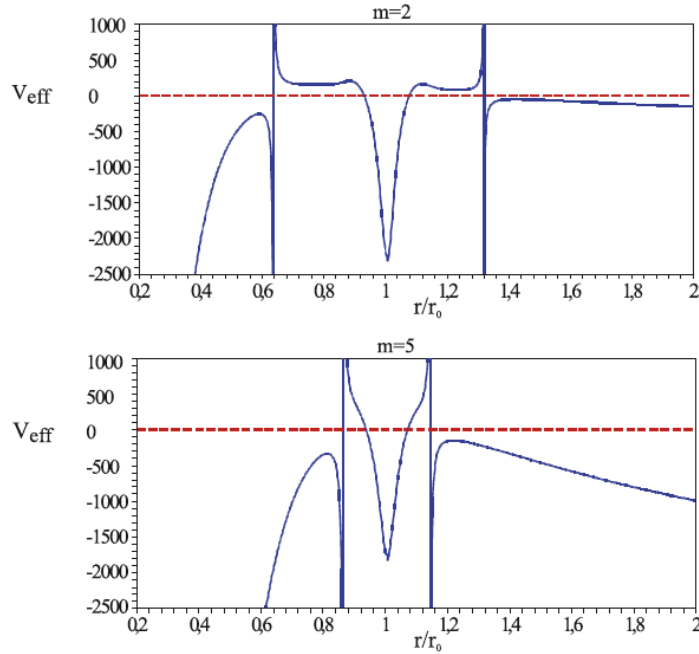


Figure 2. Effective potential for a Gaussian surface density bump of peak amplitude $\Delta\Sigma/\Sigma = 0.2$ and width $\Delta r/r = 0.05$ for $m = 2$ (upper panel) and $m = 5$ (lower panel) adapted from Meheut *et al* (2013). Waves can propagate only in the regions where $V_{\text{eff}}(r) < 0$. The large positive values of V_{eff} occur at the inner and outer Lindblad resonance radii.

The Rossby wave instability is analogous to the *plane parallel shear instability* which can be interpreted in terms of counter-propagating Rossby waves on either side of the resonance layer (r_0) and the over-reflection of waves from this resonance layer (Lindzen 1988; Harnik and Heifetz 2007). The analogy remains to be fully investigated. An interpretation of the Rossby instability as arising from the interaction of two “edge waves” on either side of the bump in $\mathcal{L}(r)$ is given by Umurhan (2010) who points out the analogy of the RWI with the *diochotron* instability (Buneman 1957; Knauer 1966) of rotating, non-neutral plasmas in a uniform magnetic field for cases where the plasma is annular with both inner and outer radii so that there are two edge waves.

The Rossby wave instability occurs because of the local wave trapping in a disc. It is related to the Papaloizou and Pringle (1984, 1985) instability where the wave is trapped between the inner and outer radii of a disc or torus.

Two-dimensional hydrodynamic simulations of the RWI instability in discs have been done by many groups beginning with Li *et al* (2001). Figure 3 from Li *et al* (2001) shows an example of the $m = 3$ vortices formed by the RWI. Three-dimensional simulations of the instability have been done by Meheut *et al* (2010, 2012a). The behavior of the Rossby wave instability is not dramatically altered in going from the 2D to 3D hydrodynamics. In 3D there are vertical (z) motions associated with the vortices, but the magnitudes of the vertical velocities are small compared with the

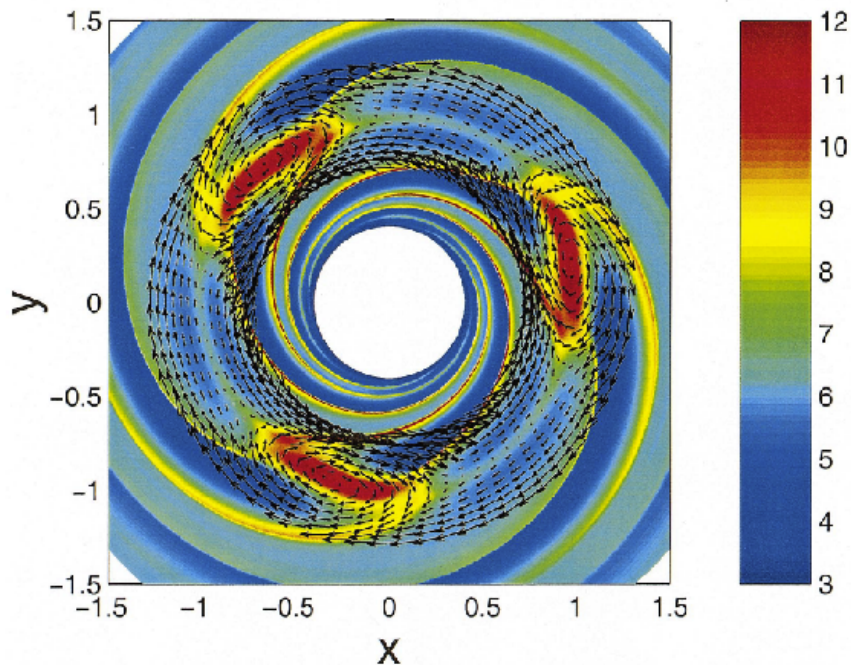


Figure 3. 2D hydrodynamic simulations of Rossby vortices in a disk adapted from Li *et al* (2001) for $m = 3$. Pressure is color-coded (in units of $10^{-3}p_0$). Arrows indicate the flow pattern near r_0 in a comoving frame moving with velocity $u_\phi(r_0)$. The vortices are *anticyclonic*, enclosing high-pressure regions. Large-scale spirals are produced as well, in connection with the vortices.

horizontal perturbation velocities. Earlier 3D simulations of vortices in stratified protoplanetary discs by Barranco and Marcus (2005) gave a more complicated picture of the vortex dynamics.

The theory of the instability in three dimensions has been developed by Meheut *et al* (2012b) and Lin (2012). A useful set of references can be found in the proceedings of a recent meeting on vortices and dust dynamics in proto-planetary discs edited by Barge and Jorda (2013).

3. Trapping of dust accretion disc vortices

Barge and Sommeria (1995) first pointed out that anticyclonic vortices in an accretion disc can act to concentrate dust particles in the flow and that this would facilitate the formation of planetesimals. This subject has been further developed in many subsequent papers (e.g., Tanga *et al* 1996; Bracco *et al* 1999; Godon and Livio 2000; Johanssen *et al* 2004; Heng and Kenyon 2010). A qualitative explanation is simple. First note that in an axisymmetric proto-stellar disc the radial force balance for the gas component is $-u_{\phi\text{gas}}^2/r = -(dp/dr)/\rho - GM_*/r^2$, where $u_{\phi\text{gas}}$ is gas velocity, p is its pressure, ρ is its density, and M_* is the mass of the central star. The pressure gradient term

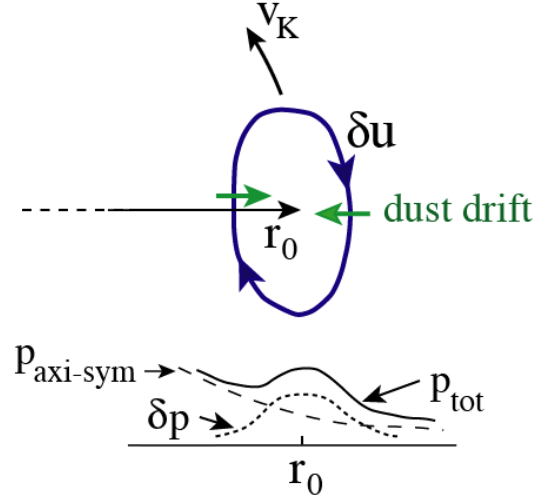


Figure 4. Sketch of an anticyclonic vortex centered at radius r_0 in a Keplerian disc at some instant of time. The velocity perturbation of the vortex is $\delta \mathbf{u}$. The lower part of the figure sketches the radial pressure variation through the vortex center.

can be estimated as $(dp/dr)/\rho \approx -c_s^2/r$, with $c_s = (p/\rho)^{1/2}$ the sound speed of the gas. Thus the gas velocity is slightly sub-Keplerian, $u_{\phi\text{gas}} \approx v_K[1 - (c_s/v_K)^2/2]$, where $v_K \equiv (GM_*/r)^{1/2}$ is the Keplerian velocity and $c_s/v_K \ll 1$ for proto-stellar discs (where typical value is $c_s/v_K = 0.05$). On the other hand the dust component of the proto-stellar disc is not affected by a pressure gradient and consequently the dust velocity is Keplerian $u_{\phi\text{dust}} = v_K$. The dust particles move slightly faster than the gas and consequently lose angular momentum by the drag from their motion through the gas. Dust particles of sizes 0.01 – 1 cm inspiral to the proto-star faster than the gas for commonly assumed disc viscosities. A rigorous 3D analysis of the dust motion in axisymmetric discs is given by Takeuchi and Lin (2002).

Consider a vortex of small radial and azimuthal extent formed by some process in a disc as sketched in Figure 4. It has velocity perturbation $\delta \mathbf{u}$ and pressure perturbation δp . In a reference frame rotating with angular rate $\Omega(r_0)$ ($\approx v_K(r_0)/r_0$), the flow approximately satisfies the geostrophic equation $(\nabla \delta p)/\rho = 2\delta \mathbf{u} \times \boldsymbol{\Omega}$, which is a balance of the pressure gradient and Coriolis forces. An *anticyclonic vortex*, with vorticity $\nabla \times \delta \mathbf{u}$ oppositely directed to $\boldsymbol{\Omega}$, has a maximum of δp at the vortex center. (A cyclonic vortex has a pressure minimum at its center.) A dust particle in the outer part of the vortex moves faster than the gas and drifts radially inward. On the other hand a dust particle in the inner part may move slower than the gas with the result that it drifts radially outward. For dust trapping the vortex must be strong enough for the radial pressure gradient to be positive for an interval inside r_0 . This gives the condition $|\delta \mathbf{u}| \gtrsim c_s^2/2v_K$, which is readily satisfied by the vortices arising from the RWI.

Dust trapping in vortices in 3D disc simulations has been studied by modeling the

dust component as a separate pressureless fluid coupled to the gas by collisions (Meheut *et al* 2012c) for dust particle sizes of 0.1 – 5 cm. The dust to gas mass fraction, initially 10^{-2} , was found to increase by a factor of order 10^2 in the centers of the vortices (Meheut *et al* 2012c). At this mass fraction the dust has a significant back reaction on the gas dynamics.

4. Vortices at the radial margins of the dead zone in disc

A bump in $\mathcal{L}(r)$ or $\Sigma(r)$ may arise at the radial boundaries of the “dead zone” (Varnière and Tagger 2006; Lyra *et al* 2009; Crespe *et al* 2011). This zone can arise from the suppression of the magneto-rotational instability (MRI, Balbus and Hawley 1991) by low ionization inside the disc (Gammie 1996). The MRI is a small length-scale instability of conducting Keplerian discs in the presence of a weak magnetic field where the magnetic pressure is less than the thermal pressure in the disc. The instability is found to give rise to magnetic turbulence with length-scales of the order of the disc thickness. In turn this turbulence provides an effective viscosity which is commonly thought to cause the accretion of matter and the outward transport of angular momentum in astrophysical discs (Balbus and Hawley 1991). Note however the possibility that the turbulent viscosity arises in hydrodynamic (non-magnetized) discs owing to the nonlinear instability in the very large Reynolds number, Rayleigh-stable Keplerian discs (specific angular momentum increasing outward) (Paoletti *et al* 2012; Bisnovatyi-Kogan and Lovelace 2001; Zeldovitch 1981). The bump in $\mathcal{L}(r)$ can give rise to exponential growth of non-axisymmetric perturbations in the vicinity of r_0 consisting of *anticyclonic* vortices. In most studies the dead zone has been modeled as radial interval of the disc with a significantly reduced turbulent viscosity compared with the outer and inner parts of the disc. This is due to the reduced action of the MRI. However, recently, Lyra and Mac Low (2012) carried out global 3D magneto-hydrodynamic (MHD) simulations of the full problem by modeling the dead zone as a region of the disc with significantly lower resistivity. They find that the RWI develops on the inner edge of the dead zone.

5. Vortices due to planet induced gap edges

The interactions of a planet with a proto-stellar disc has been studied theoretically and with 2D and 3D hydrodynamic simulations by many authors primarily because of its importance to planet migration, that is, the slow inward or outward radial motion of the planet due to transfer of angular momentum between the planet and the disc. The dependence of the migration rate and the influence of a planet on the disc (e.g., the formation of a gap in the disc) depends of course on the planet’s mass, and it was thought that the formation of a gap in the disc occurs only for planets more massive than about one-tenth of Jupiter’s mass (Lin and Papaloizou 1993). But the gap formation is sensitive also to the nonlinear steepening and shock formation of the spiral density waves generated by the planet (Rafikov 2002) as well as the turbulent viscosity of the

disc which damps the density waves (Li *et al* 2009). For sufficiently low viscosities, the shocks formed by the spiral density waves at the gap edges give rise to maxima in the inverse vortensity $\mathcal{L}(r)$ (Koller *et al* 2003; Li *et al* 2005; de Val-Borro *et al* 2007; Lin and Papaloizou 2010). This triggers the Rossby wave instability. Starting from axisymmetric conditions the simulations show the growth and saturation of several vortices ($m = 3 - 5$) which later merge to form a single vortex.

Recent high resolution 3D hydrodynamic simulations by Zhu *et al* (2014) indicate that a gap may be formed over a sufficiently long period for M_p larger than ten times the earth mass. In this work the gas component of the disc was modeled with the grid based code *Athena*, and the dust component with Lagrangian particles for a wide range of dust particle sizes (0.01 – 10² cm). The dust surface mass density in the Rossby vortices is found to increase by a factor of 10² for dust particles with $\Omega_K t_s \sim 1$, where Ω_K is the Keplerian rotation rate of the disc at r_0 , and t_s is the stopping time of the dust particle motion through the gas (proportional to the particle’s radius) (Zhu *et al* 2014). Note that in the work of Meheut *et al* (2012c), where the dust component was treated as a separate fluid, a comparable increase in the dust density was found. Analytic solutions for the dust distribution in disc vortices have been developed by Birnstiel *et al* (2013) and Lyra and Lin (2013).

Recent observations by van der Marel *et al* (2013) of the disc around the star Ophiuchus IRS 48 with the Atacama Large Millimeter Array (ALMA) have revealed a high-contrast crescent-shaped emission region in the 0.44 mm wavelength from one side of the star indicating a concentration in this region of millimeter size dust grains. The contrast ratio between the peak emission and the opposite side of the disc is $\sim 10^2$. At the same time observations at different wavelengths indicate that both the gas and the micrometer-sized dust is distributed uniformly in the disc around the star (van der Marel *et al* 2013). The asymmetric dust emission of Oph IRS 48 is modeled as a single anticyclonic Rossby vortex ($m = 1$) excited at the outer gap edge of a ~ 10 Jupiter mass planet orbiting the star at 20 AU (AU is the Sun-Earth distance, 1.5×10^{13} cm) (van der Marel *et al* 2013). The center of the vortex or dust trap is estimated as 63 AU and it is on the line through the planet and star.

6. Saturation and merging of vortices

Starting from axisymmetric conditions, a bump in $\mathcal{L}(r)$ of amplitude larger than a critical value will lead to the exponential growth of a Rossby wave for a particular azimuthal mode number (typically, $m = 3 - 5$) (Lovelace *et al* 1999). The exponential growth is predicted to cease at the time when the circulation or trapping time of a fluid particle in one of the vortices, τ_T , is of the order of the growth-time of the instability, ω_i^{-1} (Lovelace *et al* 2009). This is because the axisymmetric fluid motion assumed in the instability calculation (Lovelace *et al* 1999) is inapplicable for times $\gtrsim \tau_T$. An analogous saturation conditions is well-known in plasma physics where it was first used to explain the saturation of the two-stream instability (O’Neil 1965; Krall and Trivelpiece 1973). A

systematic study of the Rossby wave saturation with 2D and a sample 3D hydrodynamic simulations finds that the exponential growth saturates when $\tau_T \lesssim \omega_i^{-1}$ with $\tau_T \approx 2/|\omega_v|$ where $\omega_v = |\nabla \times \delta \mathbf{u}|$ is the vorticity of the Rossby vortex (Meheut *et al* 2013). The saturation is found to occur in about 5 – 10 orbital periods at the radius of the bump (Meheut *et al* 2013).

An axisymmetric bump in the inverse vortensity $\mathcal{L}(r)$ may be maintained at the edge of a disc’s dead zone or at the edges of a gap formed in the disc by a planet. The maintenance of the bump can allow the continuous driving of the Rossby vortices for the lifetime of the disc. In the absence of a mechanism for maintaining the bump, long-time 3D hydrodynamic simulations show that the Rossby vortices persist for times of the order of 10^2 orbital periods at the radius of the bump (Meheut *et al* 2012a). For longer times the bump in \mathcal{L} is spread out in radius and reduced in amplitude below the instability threshold. The vortices do not show measurable radial migration.

The long-time simulations show that an initial multiple vortex pattern ($m = 3 - 5$) evolves by vortex merging to give a single vortex ($m = 1$) (Meheut *et al* 2012a). A detailed theoretical analysis of the stability of a single elliptical Kida vortex model (1981) has been carried out by Leseur and Papaloizou (2009) with the result such vortices are unstable except for azimuthally elongated vortices which have azimuthal half-widths ($r_0 \Delta \phi$) longer than 4 times the radial half-width (Δr) but with this ratio less than 6.

7. Influence of a large-scale magnetic field on vortices

The influence of a large-scale magnetic field on the Rossby wave instability has been investigated by Tagger and collaborators (Tagger and Pellat 1999; Tagger and Varnière 2006; Tagger and Melia 2006) and others (Yu and Li 2009; Yu and Lai 2013). Strong, kilo-Gauss, dipole and higher multipole moment magnetic fields are observed in proto-stars (e.g., Yang and Johns-Krull 2011). The stellar magnetic field penetrates the proto-stellar disc to different radial extents depending mainly on the stellar field strength and the disc accretion rate (Lii *et al* 2012). This large-scale field in the inner disc can drive the high velocity jets observed owing to the gradient of the wound-up toroidal magnetic fields (Lii *et al* 2012). At the same time the toroidal magnetic field collimates the jet. Large-scale magnetic fields are also thought to be responsible for the relativistic jets observed to come from accretion discs around black holes ranging from stellar mass to supermassive ($\sim 10^{10}$ solar mass). In the presence of a large-scale, vertical magnetic field $B_z(r)$, Tagger and collaborators find that the inverse vortensity of equation (1) may be superceded by the quantity $(B_z/\Sigma)^2 \mathcal{L}$ depending on the value of $|B_z|/\Sigma$.

A distinguishing aspect of the magnetic RWI is the prediction of the outflow of energy and angular momentum via Alfvén waves from the vortices into the disc’s corona (Tagger and Pellat 1999; Tagger and Varnière 2006). The outflows from the rotating vortices could explain the quasi-periodic oscillations (QPOs) observed in the X-ray emissions of low-mass X-ray binaries (van der Klis 2006). A further promising application of the magnetic RWI is to modeling the quasi-periodic (~ 20 min.) near

infra-red and X-ray emission from material orbiting the super massive black hole Sagittarius A* ($M \sim 3 \times 10^6$ solar masses) in the center of our Galaxy (Tagger and Melia 2006). The authors propose that low angular momentum clouds episodically fall into the vicinity of the black hole and the gas becomes trapped and circularized by viscosity at ~ 30 Schwartzchild radii ($r_S = 2GM/c^2 \sim 10^{12}$ cm) from the black hole. This event would naturally produce a pronounced bump in the disc surface density and $\mathcal{L}(r)$, strong Rossby wave growth at the trapping radius, and magnetically driven outflows with a quasi-period similar to that observed. Note that Vincent *et al* (2013) find quasi-periodic oscillations in the thermal emission from the inner regions of *non-magnetized* discs around black holes. They find the RWI in from 2D and 3D simulations using the *AMRVAC* code.

A different type of Rossby wave instability was found by Lovelace *et al* (2009) in the strongly non-Keplerian magnetized region of a disk where $d\Omega/dr > 0$. For a Keplerian disc, $d\Omega/dr = -(3/2)\Omega/r$. This region occurs when an accretion disc encounters the magnetosphere of a slowly rotating star (Romanova *et al* 2008). This Rossby mode was proposed as an explanation (Lovelace *et al* 2009) of the observed twin kilo-Hertz QPOs (van der Klis 2006). Evidence for the occurrence of this Rossby mode with $m = 2$ and $d\Omega/dr > 0$ has been found in the power spectral density plots of the global 3D MHD simulations of waves in discs around rotating magnetized stars with misaligned dipole magnetic fields using the *Cubed Sphere* code (Romanova *et al* 2013).

8. Vortices in self-gravitating discs

The self-gravity of disc can have an important influence on the Rossby wave instability in proto-planetary discs, black hole discs, as well as disc galaxies. The RWI, earlier termed the “negative mass instability” (Lovelace and Hohlfield 1978), was in fact developed for spiral or disc galaxies which are self-gravitating systems of stars and gas. The rotation curves the disc galaxies are *not* Keplerian, but “flat” because they have $u_\phi \approx \text{const}$ for a large range of radial distances outside their central nuclear regions. For disc galaxies $\mathcal{L} \rightarrow \sigma\Omega/\kappa^2$ (Lovelace and Hohlfield 1978), where κ is the radial epicyclic angular frequency given below equation 3. The RWI in disc galaxies consisting predominantly of stars has been observed and studied in many different cases using N -body simulations (Sellwood and Kahn 1991; Sellwood 2012; Sellwood 2013). Only a small bump or depression in $\mathcal{L}(r)$ leads to the growth of a global disc mode (Sellwood 2013). When the self-gravity of the disc is strong, the RWI is observed to occur at radii where \mathcal{L} is a *minimum* rather than a maximum (Sellwood and Kahn 1991; Sellwood 2012, 2013) as predicted by Lovelace and Hohlfield (1978).

In proto-stellar discs, the influence of the self-gravity of the gas and dust on vortices generated by giant Jupiter-mass scale planets have been studied in several recent simulation studies (Lyra *et al* 2009; Lin and Papaloizou 2011). Lyra *et al* (2009) use a thin disc, 2D model for the gas and dust with the gas described by hydrodynamic equations and the dust described by a large number of Lagrangian particles (typically

10^5) using the *Pencil* code. The dust and gas are coupled by an analytic drag force model which allows for a wide range of particle sizes and gas conditions. The self-gravity is calculated using a Fourier transform method. Significant dust accumulation is found to occur at the Lagrange points of the planet as well as in the vortices generated at the edges of the planet induced gap in the disc. The analysis of Lin and Papaloizou (2011) is also for thin discs using analytic methods and 2D hydrodynamic simulations with the *Fargo* code. The vortices studied were those arising from the planet induced bumps in $\mathcal{L}(r)$ at the gap edges. The analytic theory and simulations show that the Rossby instability is stabilized for low mode numbers (m) as the disc mass is increased.

A simpler problem is treated by Lovelace and Hohlfeld (2013) where an analytic calculation is made of the stability of a bump or depression in $\mathcal{L}(r)$ in a thin Keplerian disc in the absence of planets. The results are in agreement with Lovelace and Hohlfeld (1978). The key quantities determining the stability/instability are found to be: (1) The parameters of the bump (or depression) in the disc surface density. (2) The Toomre $Q = \kappa c_s (\pi G \Sigma)^{-1}$ parameter of the disc with c_s is the sound speed in the disc (Toomre 1964; Safronov 1960) where a non-self-gravitating disc has $Q \gg 1$. And, (3) the dimensionless azimuthal wavenumber of the perturbation $\bar{k}_\phi = mQh/r_0$, where h is the half-thickness of the disc. For discs stable to axisymmetric perturbations ($Q > 1$), the self-gravity has a significant role for $\bar{k}_\phi < \pi/2$ or $m < (\pi/2)(r_0/h)Q^{-1}$; instability may occur for a depression or groove in the surface density if $Q \lesssim 2$. For $\bar{k}_\phi > \pi/2$ the self-gravity is not important, and instability may occur at a bump in the surface density. Thus, for all mode numbers $m \geq 1$, the self-gravity is unimportant for $Q > (\pi/2)(r_0/h)$. This review does not consider the instability of self-gravitating gas discs for conditions where the gas cooling is important (Gammie 2001).

9. Conclusion

Recent research on vortices in astrophysical discs is evolving particularly rapidly owing to the completion of the ALMA infra-red telescope array which allows for the first time the mapping of the distribution of gas and dust grains in the discs of nearby proto-planetary systems. Observations by van der Marel *et al* (2013) with ALMA of a crescent shaped dust concentration in the disc of a proto-star is most simply interpreted as a large mass of dust trapped in the high pressure region of an anticyclonic vortex. At the same time increasingly sophisticated codes have been developed for simulating the 3D flow of gas and dust in discs (e.g., Zhu *et al* 2014).

Acknowledgments

We thank Professor Michael Mond of Ben-Gurion University and Professor Alexander Oron of the Technion for the invitation to the meeting *Bifurcations and Instabilities in Fluid Mechanics* held at the Technion in Haifa Israel in July 2013. Further, we thank Dr. Orkan Umurhan for valuable discussions on Rossby vortices.

References

- Balbus, S.A., and Hawley, J.F. 1991, *ApJ*, 376, 214
- Barge, P., and Jorda, L. (eds.) 2013, *Instabilities and Structures in Proto-Planetary Disks*, EPJ Web of Conferences 46, 2013
- Barge, P., and Sommeria, J. 1995, *A&A*, 295, L1
- Barranco, J.A., and Marcus, P.S. 2005, *ApJ*, 623, 1157
- Birnstiel, T., Dullemond, C.P., and Pinilla, P. 2013, *A&A*, 550, L8
- Bisnovatyi-Kogan, G.S., and Lovelace, R.V.E. 2001, *New Astronomy Reviews*, 45, 663
- Bracco, A., Chavanis, P.H., Provenzale, A., and Spiegel, E.A. 1999, *Phys. Fluids*, 11, 2280
- Brekhovskikh, L. M., and Goncharov, V. 1993, *Mechanics of Continua and Wave Dynamics* (Berlin: Springer), pp 246-252
- Buneman, O. 1957, *J. Electronics and Control*, 3, 507
- Chelton, D.B., and Schlax, M.G. 1996, *Science*, 272, 234
- Crespe E., Gonzalez J.-F., and Arena S. E., 2011, in SF2A-2011: Proceedings of the Annual meeting of the French Society of Astronomy and Astrophysics, G. Alecian, K. Belkacem, R. Samadi, and D. Valls-Gabaud, eds., (Societe Francaise d'Astronomie et d'Astrophysique (SF2A)), pp. 469-473
- de Val-Borro, M., Artymowicz, P., D'Angelo, G., and Peplinski, A. 2007, *A&A*, 471, 1043
- Gammie, C.F. 1996, *ApJ*, 457, 355
- Gammie, C.F. 2001, *ApJ*, 553, 174
- Godon, P., and Livio, M. 2000, *ApJ*, 537, 396
- Harnik, N., and Heifetz, E. 2007, *J. Atmospheric Sciences*, 64, 2238
- Heng, K., and Kenyon, S.J. 2010, *MNRAS*, 408, 1476
- Johanssen, A., Andersen, A.C., and Brandenburg, A. 2004, *A&A*, 417, 361
- Kida, S. 1981, *Phys. Soc. Japan J.*, 50, 3517
- Knauer, W. 1966, *J. Appl. Phys.*, 37, 602
- Koller, J., Li H., and Lin D. N. C. 2003, *ApJ*, 596, L91
- Krall, N., and Trivelpiece A. 1973, *Principles of Plasma Physics*, McGraw-Hill, New York, p. 536
- Lai, D., and Tsang ,D., 2009, *MNRAS*, 393, 979
- Leseur, G., and Papaloizou, J.C.B. 2009, *A&A*, 498, 1
- Li, H., Colgate, S. A., Wendroff, B., and Liska, R. 2001, *ApJ*, 551, 874
- Li, H., Finn, J.M., Lovelace, R.V.E., and Colgate, S.A. 2000, *ApJ*, 533, 1023
- Li, H., Li, S., Koller, J. Wendroff, B.B., Liska, R., Orban, C.M., Liang, E.P.T., and Lin, D. N. C. 2005, *ApJ*, 624, 2003
- Li, H., Lubow, S.H., Li, S., and Lin, D.N.C. 2009, *ApJ*, 690, L52
- Lii, P., Romanova, M.M., and Lovelace, R.V.E. 2012, *MNRAS*, 420, 2020
- Lin, D.N.C., and Papaloizou, J.C.B. 1993, in *Protostars and Planets III*, eds. E.H. Levy and J.I. Lunine, (Univ. of Arizona Press: Tuscon), 749
- Lin, M.-K., 2012, *ApJ*, 754, 21
- Lin, M.-K., and Papaloizou, J.C.B. 2010, *MNRAS*, 405, 1473
- Lin, M.-K., and Papaloizou, J. C. B. 2011, *MNRAS*, 415, 1426
- Lindzen, R.S. 1988, *Pure Appl. Geophys.*, 126, 103
- Lindzen, R.S. 2005, *Dynamics in Atmospheric Physics* (Cambridge: Cambridge Univ. Press), pp 222-233
- Lovelace, R.V.E., Li, H., Colgate, S.A., and Nelson, A.F. 1999, *ApJ*, 513, 805
- Lovelace, R.V.E., and Hohlfeld, R.G. 1978, *ApJ*, 221, 51
- Lovelace, R.V.E., and Hohlfeld, R.G. 2013, *MNRAS*, 429, 529
- Lovelace R. V. E., Turner L., and Romanova M. M., 2009, *ApJ*, 701, 225
- Lyra, W., Johansen, A., Zsom, A., Klahr, H., and Piskunov, N. 2009, *A&A*, 497, 869
- Lyra, W., and Lin, M.-K. 2013, *ApJ*, 775, article id. 17, pp. 1-10 (arXiv:1307.377)
- Lyra, W., and Mac Low, M.M. 2012, *ApJ*, 756, 62

- Marcus, P.S. 1993, *Ann. Rev. Astron. and Astrophys.*, 31, 523
- Meheut, H., Casse, F., Varnière, P., and Tagger, M. 2010, *A&A*, 516, A31
- Meheut, H., Keppens, R., Cassee, F., and Benz, W. 2012a, *A&A*, 542, A9
- Meheut, H., Yu, C., and Lai, D. 2012b, *MNRAS*, 422, 2399
- Meheut, H., Meliani, Z., Varniere, P., and Benz, W. 2012c, *A&A*, 545, A134
- Meheut, H., Lovelace, R.V.E., and Lai, D. 2013, *MNRAS*, 430, 1988
- O’Neil, T. 1965, *Phys. Fluids*, 8, 2255
- Paoletti, M.S., van Gils, D.P.M., Dubrulle, B., Sun, C., Lohse, D., and Lathrop, D.P. 2012, *A&A*, 547, A64
- Papaloizou, J. C. B., and Pringle, J. E. 1984, *MNRAS*, 208, 721; ——— 1985, *MNRAS*, 213, 799
- Rafikov, R.R. 2002, *ApJ*, 572, 566
- Romanova, M. M., Kulkarni, A. K., and Lovelace, R. V. E. 2008, *ApJ*, 673, L171
- Romanova, M. M., Ustyugova, G. V., Koldoba, A. V., and Lovelace, R. V. E. 2013, *MNRAS*, 430, 699
- Rossby C.-G. and Collaborators 1939, *Journal of Marine Research*, 2, 38
- Safronov, V.S. 1960, *Ann. Astrophys.*, 23, 982
- Sellwood, J.A., and Kahn, F.D. 1991, *MNRAS*, 250, 278
- Sellwood, J.A. 2012, *ApJ*, 751, 44
- Sellwood, J.A. 2013, Chap. 18, “Dynamics of Disks and Warps,” in *Planets, Stars and Stellar Systems Vol. 5*, eds: Oswald, T. D. and Gilmore, G., (ISBN 978-94-007-5611-3. Springer Science+Business Media Dordrecht), p. 923 (arXiv: 1006.4855)
- Tagger, M., 2001, *A&A*, 380, 750
- Tagger, M., and Melia, F. 2006, *ApJL*, 636, L33
- Tagger, M., and Pellat, R. 1999, *A&A*, 349, 1003
- Tagger, M., and Varnière, P. 2006, *ApJ*, 652, 1457
- Takeuchi, T., and Lin, D.N.C. 2002, *ApJ*, 581, 1344
- Tanga, P., Babiano, A., Dubrulle, B., & Provenzale, A. 1996, *Icarus*, 121, 158
- Toomre, A. 1964, *ApJ*, 139, 1217
- Tsang, D., and Lai, D., 2008, *MNRAS*, 387, 446
- Umurhan, O.M. 2010, *A&A*, 521, A25
- van der Klis, M. 2006, in *Compact Stellar X-Ray Sources*, ed. W. H. G. Lewin and M. van der Klis (Cambridge: Cambridge Univ. Press), 39
- van der Marel, N., van Dishoeck, E.F., Bruderer, S., Birnstiel, T., Pinilla, P., Dullemond, C.P., van Kempen, T.A., Schmalzl, M., Brown, J.M., Herczeg, G.J., Mathews, G.S., and Geers, V. 2013, *Science*, 340, 1199, (arXiv:1306.176)
- Varnière, P., and Tagger, M. 2006, *A&A*, 446, L13
- Vincent, F.H., Meheut, H., Varnière, P., and Paumard, T. 2013, *A&A*, 551, A54
- Yang H., and Johns-Krull C. M., 2011, *ApJ*, 729, 83
- Yu, C., and Lai, D. 2013, *MNRAS*, 429, 2748
- Yu, C., and Li, H. 2009, *ApJ*, 702, 75
- Zeldovich, Y.B. 1981, *Proc. Roy. Soc. Lond.*, A, 374, 299
- Zhu, Z., Stone, J.M., Rafikov, R.R., and Bai, X. 2014, *ApJ*, 785, article id. 122